

AperTO - Archivio Istituzionale Open Access dell'Università di Torino

Experimental characterization and numerical modeling of the compressive mechanical behavior of hazelnut kernels

This is the author's manuscript

Original Citation:

Availability:

This version is available <http://hdl.handle.net/2318/1526763> since 2015-10-21T11:32:06Z

Published version:

DOI:10.1016/j.jfoodeng.2015.06.037

Terms of use:

Open Access

Anyone can freely access the full text of works made available as "Open Access". Works made available under a Creative Commons license can be used according to the terms and conditions of said license. Use of all other works requires consent of the right holder (author or publisher) if not exempted from copyright protection by the applicable law.

(Article begins on next page)



UNIVERSITÀ DEGLI STUDI DI TORINO

This Accepted Author Manuscript (AAM) is copyrighted and published by Elsevier. It is posted here by agreement between Elsevier and the University of Turin. Changes resulting from the publishing process - such as editing, corrections, structural formatting, and other quality control mechanisms - may not be reflected in this version of the text. The definitive version of the text was subsequently published in:

Journal of Food Engineering 166 (2015) 364–369; [dx.doi.org/10.1016/j.jfoodeng.2015.06.037](https://doi.org/10.1016/j.jfoodeng.2015.06.037)

You may download, copy and otherwise use the AAM for non-commercial purposes provided that your license is limited by the following restrictions:

- (1) You may use this AAM for non-commercial purposes only under the terms of the CC-BY-NC-ND license.
- (2) The integrity of the work and identification of the author, copyright owner, and publisher must be preserved in any copy.
- (3) You must attribute this AAM in the following format: Creative Commons BY-NC-ND license (<http://creativecommons.org/licenses/by-nc-nd/4.0/deed.en>), <http://www.sciencedirect.com/science/article/pii/S0260877415002927>

1 **Experimental characterization and numerical modeling of the compressive mechanical**
2 **behavior of hazelnut kernels**

3

4 Cristiana Delprete¹, Simone Giacosa², Emanuele Raviolo¹,
5 Luca Rolle², Raffaella Sesana^{1*}

6

7 ¹Politecnico di Torino, Department of Mechanical and Aerospace Engineering (DIMEAS), Corso Duca degli Abruzzi 24, 10129
8 Torino, Italy.

9 ² Università di Torino, Dipartimento di Scienze Agrarie, Forestali e Alimentari (DISAFA), Largo Paolo Braccini 2, 10095
10 Grugliasco (TO), Italy.

11

12 **Abstract**

13

14 The evaluation of mechanical properties of hazelnuts has been developed over the past years
15 mainly to optimize industrial processes. The aim of this study is to reproduce the compressive
16 behavior of hazelnut kernel obtained by experimental and numerical activities; the
17 contribution of pellicle influence to the mechanical behavior is also analyzed.

18 The experimental activity is aimed to measure the mechanical properties of hazelnut kernel
19 and to obtain a model calibration based on experimental data analysed by statistical
20 approach. The finite element models of hazelnut kernels are implemented and a set of
21 numerical compression tests are simulated; the comparison of experimental and numerical
22 responses is shown.

23

24 **Keywords:** Hazelnut kernel, mechanical properties, finite element model

25

26 **1. Introduction**

27 The hazelnut *Corylus avellana L.* is native of an area that stretches from Europe to south west
28 Asia and has been introduced in USA (California State) and several other countries around the
29 world. Turkey is the largest producer of hazelnuts in the world with approximately 75% of
30 worldwide production, followed by Italy, USA and Spain (FAO, 2014).

31 The nut kernel is the edible part of the hazelnut. Many studies have been conducted
32 regarding its internal structure, some of them dating back to the first years of the XX century
33 (Winton, 1906; Young, 1912). The edible kernel is covered by a removable thin fibrous
34 pellicle, with the internal tissue of the cotyledons consisting of parenchyma cells separated by
35 very small intercellular spaces (Young, 1912).

36 The hazelnut kernel is widely used in the food industry as fruit, grounds and in form of
37 flour. The roasting process is used to achieve an optimal flavor development and intensity of
38 taste, as for it modifies the physical, chemical and sensory characteristics.

39 The evaluation of mechanical properties of hazelnuts (whole fruit, shell, kernel) has been
40 developed over the past years with the objectives to obtain industrial processes and improve
41 the use of hazelnuts as food ingredient. The easiness to break and to remove the nut shell was
42 evaluated on Turkish varieties (Güner et al., 2003; Ozdemir and Akinci, 2004; Ercisli et al.,
43 2011) and also on nut varieties intended for fresh table consumption (Valentini et al., 2006).
44 Nut shell characteristics, such as hardness and thickness, were measured and correlated to
45 the biological cycle of the nut weevil of *Curculio nucum* (*Coleoptera: Curculionidae*) pest and to
46 the damage by its larvae (Guidone et al., 2007) stress the importance of physical properties
47 evaluation.

48 The physical characteristics of the hazelnut kernel have an important role on the crispness
49 and crunchiness sensory parameters especially on the roasted nuts (Saklar et al., 1999) and
50 the water activities have direct effects on mechanical characteristic (Borges and Peleg, 1997).
51 The overall quality is influenced by oxygen and relative humidity contents during the product
52 storage (Ghirardello et al., 2013). Di Matteo et al. (2012) evaluated also some mechanical
53 properties of chemical-peeled hazelnut kernels, such as firmness and rigidity, to study an
54 original industrial process to improve the kernel pellicle removal. A mechanical
55 characterization of whole nut, kernel and shell was conducted (Delprete and Sesana, 2014) in
56 order to aid the design and construction of selecting machines.

57 The main aim of this study is to obtain, by experimental and numerical activities, the model
58 of the compressive behavior of hazelnut kernel and to investigate the role of the pellicle
59 coating and roasting process; the here investigated variety of hazelnut is the *Tonda Gentile*
60 *Trilobata*.

61 The present study measures the mechanical properties of the kernel material, raw and
62 roasted, selects and calibrates the proper constitutive material model for numerical
63 simulations, and investigates the behavior of the whole hazelnuts in the same experimental
64 conditions (raw and roasted). Finally the research identifies the average value of the
65 investigated mechanical parameters, the variability of the measurements and the influence of
66 the number of the specimens within a single sample. The implementation and validation of a
67 numerical finite element (FE) model of hazelnut based on geometric and material data is
68 reported.

69

70 2. Materials and methods

71 Experiments were carried out to obtain the empirical data of material behavior.

72 The geometry of real kernel has been computed by means of TAC scanning of four kernels and
73 this has been used to define a numerical modeling. Material calibration data has been derived
74 from experimental test activity on specimens obtained from the same four kernels.

75

76 2.1. Experimental tests

77 The hazelnut sample was composed of about 5 kg of conform and raw *Tonda Gentile Trilobata*
78 (formerly known as *Tonda Gentile delle Langhe*) Italian autochthonous cultivar (2013
79 harvest).

80 The moisture content, determined according to the AOAC 925.40 method (AOAC, 2000), was
81 of $4.45\% \pm 0.57\%$ w.b.

82 Geometric parameters and mass of kernels were acquired as described in a previous work
83 (Delprete and Sesana, 2014).

84 According to χ^2 test and normal distribution test, the samples distributions were checked to
85 be normal. By means of Chauvenet test (Montgomery et al., 2001) measurements anomalies
86 were excluded from data processing. Minimum sample size was identified by means of
87 plotting percent relative deviation vs specimen number, selecting the sample size
88 corresponding to percent relative deviation settling to a steady value.

89 For roasting process, about 2 kg hazelnuts were put in oven roasted at 140 °C of roasting
90 temperature during 30 minutes (Donno et al., 2013). Moisture content of roasted hazelnuts, at
91 the time of analysis, was $2.40\% \pm 0.31\%$ w.b.

92 Compressive tests were performed based on the previous studies (Delprete and Sesana, 2014;
93 Valentini et al., 2006; Ghirardello et al., 2013).

94 In particular, a reference system has been defined on the kernel indicating three main
95 directions and dimensions as reported in Figure 1. The testing machine is a TA.XTplus texture
96 analyzer (Stable Micro Sytems, Godalming, UK), with loading speed 6 mm/min (down plate
97 moving). For all tests, the average curve was calculated by Matlab R2010b software, by means
98 of dedicated routines developed for the present research activity. Each considered sample is
99 composed consisted of at least 50 specimens.

100 To optimize the experimental conditions that allow the best monitoring of the measurement
101 changes, (according to Torchio, et al., 2012), and to evaluate the influence of the sample size
102 on the variability in the measurements, the optimum sample size was assessed representing

103 the relative standard deviation (RSD) values against the number of measurements for each
104 parameter. The stabilization of the RSD assessed the minimum sample size.

105 The first test sample (Sample 1) is composed of 50 just shelled raw hazelnut kernels while
106 the second (Sample 2) is composed of 50 manual peeled raw hazelnut kernels; that is, in the
107 former case the kernels are provided with pellicle while, in the latter one, the pellicle has been
108 removed by a careful hand scraping procedure. In particular, by means of a sharp razor and a
109 lens, the pellicle has been carefully removed, taking care of not cutting away kernel material.
110 In both cases the kernels are compressed along the A direction (Delprete and Sesana, 2014).
111 In Figure 2 the test setup is presented.

112
113 **Figure 1: Hazelnut shell and kernel main dimensions.**

114
115 **Figure 2: Kernel compression along A axis, experimental setup.**

116
117 The third test sample (Sample 3) is composed of 50 roasted hazelnut kernels; pellicle was
118 removed, as the roasting procedure makes it to detach from the kernels. As in the previous
119 cases, the testing procedure consists in a compression along the A direction.
120 From these three sets of tests, the force-displacement curves were acquired, the average
121 maximum load (\bar{L}_{kf}) to break the hazelnuts and the slope (stiffness \bar{K}) of the linear part of
122 the compression curve were calculated for each specimen within the corresponding sample. It
123 has to be noted that the hazelnut failure force was defined as the force needed for the
124 separation of the two cotyledons (Figure 3). For each of these parameters, χ^2 test was done to
125 verify the normality of distributions and the relative standard deviation analysis was done to
126 optimize the sample size.

127
128 **Figure 3: Compression failure of hazelnut kernel: cotyledon separation.**

129
130 The fourth (Sample 4) and fifth (Sample 5) test samples are composed of raw and roasted
131 kernel specimens, respectively (Figure 4 a), undergoing compression test (Figure 4b). The
132 specimens are cylindrical, 5 mm high and 5 mm diameter, and they are obtained by means of
133 two dedicated tools: the first tool cuts a slice (thickness of 5 mm) from the kernel with two
134 parallel surfaces, the second tool is a circular blade of 5 mm diameter and it cuts a cylinder
135 from the kernel slice. Cylinders were cut without taking into account of the direction as the
136 kernel material results to be hygroscopic (Delprete and Sesana, 2014). The kernel specimens

137 were obtained from each of the four described groups of hazelnuts, basing based on their
138 kernel conformity.

139

140

Figure 4: Kernel specimens a) and specimens compression setup b).

141

142 From these two sets, the stress-strain curves were acquired, the average maximum stress to
143 break the specimens (UCS), the slope (elastic modulus \bar{E}_k) of the linear part of the curves
144 and the knee stresses (σ_k) were calculated (Delprete and Sesana, 2014).

145 The sixth experimental sample was concerned about four raw kernels without pellicle. By
146 using computed tomography analysis (CTA) these four raw kernels were scanned and the
147 actual geometry including the inner cava was digitalized. The four raw kernels were
148 compressed until cotyledon separation and, from the cotyledons of each of them, cylindrical
149 kernel specimens were obtained and compressed. Results obtained were processed to obtain
150 the above-mentioned parameters, but without average calculation. hen, These results have
151 been compared with the results of previous samples to check if they could belong to the same
152 range of results.

153 The corresponding constitutive curves were used to calibrate the numerical FE models of
154 each kernel. Finally the simulation of compression of the kernel was run.

155

156 2.2. Numerical modeling

157 The numerical analysis was carried out with the commercial finite element software ABAQUS
158 6.11-1.

159 Compression tests showed that the hazelnut kernel is elastic and isotropic and then the
160 material constitutive model selected for the FE model is elastic isotropic. To calibrate the
161 model, the elastic modulus was measured following the procedure described in (Delprete and
162 Sesana, 2014). The Poisson's ratio was not measured and, as a first approximation, it was kept
163 constant to 0.3.

164 Geometry information was acquired by CTA; the output STL file discretizes the outer surface
165 and the internal cavity surface with 0.4 mm resolution. Due to the extremely large number of
166 elements, a re-mesh operation was carried out; moreover the space between the inner and
167 the outer surface was filled by 4-node linear tetrahedron elements. Table 1 gives a
168 comparison of the number of nodes and elements for each hazelnut kernel.

169

170

Table 1: Elements and nodes of numerical hazelnuts.

171
172 The simulation aims to reproduce the experimental tests, in which the hazelnuts are
173 compressed between two steel plates. Two infinite stiff plates simulate these plates because
174 the elastic modulus of steel is four orders of magnitude greater than that of the hazelnuts; this
175 choice guarantees a lower computational time.

176 A zero displacement boundary condition is imposed on the lower plate and a 2 mm boundary
177 condition on the upper plate.

178 Some nodes in the lower part of the hazelnut mesh were constrained to the lower plate by low
179 stiffness spring elements to ensure solution convergence. Volume force corresponding to
180 gravity effect is imposed on the whole model.

181 The analysis type is static and the numerical implicit procedure is based on Newton-Raphson
182 method, which allows obtaining solutions for non-linear problems. In this case the source of
183 nonlinearity is not represented by the material but by the geometry, whose changes during
184 the simulation are not negligible.

185 The contact formulation is based on a surface-to-surface discretization, so contact conditions
186 are enforced over regions around slave nodes rather than only at individual nodes (ABAQUS
187 Analysis User's Manual). The plates are the master surfaces while the hazelnut is the slave
188 surface.

189 The contact property between the plates and the hazelnut is assumed as Coulomb friction
190 model with constant coefficient $\mu = 0.3$.

191

192 **3. Results and discussion**

193

194 **3.1. Experimental testing**

195 **3.1.1. Physical properties**

196 The mass measurement distribution of hazelnut kernels can be assumed as a normal
197 distribution (positive χ^2 test, 85% confidence level); the corresponding average and standard
198 deviation values and the sample size are reported in Table 2.

199 For what concerns geometric measurements, statistical analysis was run on A/B , C/B and C/A
200 values (Delprete and Sesana, 2014). The distribution of these ratios can be assumed as a
201 normal distribution (positive χ^2 test, 85% confidence level) with average values and standard
202 deviations reported in Table 2.

203 The obtained mass and geometric results show a distribution which is coherent with
204 analogous results described in (Delprete and Sesana, 2014).

205

206

Table 2: Average values and standard deviations of physical and geometrical measurements on the specimen samples.

207

208

209

3.1.2. Whole kernel mechanical properties

210

In Figure 5 experimental force-displacement curves of raw kernels with and without pellicle (Sample 1 and 2 respectively) are reported along with the average calculated curves.

211

212

Stiffness distribution of raw kernels with pellicle can be assumed as a normal distribution and

213

the corresponding values are reported in Table 3; also the load to failure distribution gives a

214

positive χ^2 test and so can be considered normal. For both these parameters it is possible to

215

define a minimum sample size by means of the stabilization of the percent relative standard

216

deviation. The 70% of the sample presents a defined failure point; for the remaining

217

specimens the corresponding point is not recognizable on the curves.

218

219

220

Figure 5: Force-displacement raw kernel curves with (blue) and without (red) pellicle. Average curves are respectively the green and the cyan ones.

221

222

223

For what concerns Samples 2 and 3, that is raw and roasted kernels without pellicle, both

224

stiffness and load to failure are normally distributed; the mean and standard deviation values

225

are reported in Table 3. The 64% of the Sample 2 and the 58% of the Sample 3 present a

226

defined failure point. In both cases it is possible to define a minimum sample size both for the

227

stiffness and for the load to failure because of the stabilization of the percent relative standard

228

deviation.

229

In Figure 6 experimental force-displacement curves of roasted kernels are reported along

230

with the average calculated curve.

231

232

233

Figure 6: Force-displacement roasted kernel curves with average curve (white).

234

235

The normality of the stiffness distributions leads to the definition of a 95% confidence level

236

interval. In Figure 7 three intervals are shown, corresponding to raw kernels (with and

237

without pellicle) and roasted kernels. The two raw kernel intervals have an intersection but a

238

consistent part of the raw with pellicle interval extends above the raw without pellicle one. On

239

the other side the lower part of the raw without pellicle interval lies below the raw with

240 pellicle one. So the presence of the pellicle has an important effect on the compressive
241 behavior of the kernel; in particular, as it is shown in Figure 5, it increases the average
242 stiffness.

243

244

245 **Figure 7: Raw kernels with (blue continuous lines) and without (red continuous lines) pellicle and roasted without**
246 **(black continuous lines) pellicle: 95% stiffness values limits.**

247

248 The roasted kernel interval is just a little greater than the raw with-pellicle interval and so the
249 corresponding average curves are very similar. This means that the material properties have
250 increased due to baking; in particular the roasted kernels have obtained almost the same
251 average stiffness as the raw with pellicle kernels.

252 These results show a distribution which is coherent with analogous results described in
253 (Delprete and Sesana, 2014). The numerical values ~~varied are therefore different~~ as a
254 different moisture level is present in the examined sample and it is well known (Koyuncu et
255 al., 2004; Guner et al., 2003) that for wood and shells this property influences the mechanical
256 properties.

257

258

Table 3: Mechanical properties measurements on the whole kernel samples.

259

260 **3.1.3. Kernel specimens mechanical properties**

261 For the two Samples 4 and 5 the stiffness distributions can be considered normal. The average
262 value, the standard deviation and the minimum sample size are shown in Table 4.

263

264

Table 4: Mechanical properties measurements on the kernel specimen samples.

265

266 Experimental stress-strain curves can show, in the range 0-1.5 mm displacement, two
267 distinctive trends; the first consists in a clear change of slope of the curve, the second in the
268 presence of a maximum. As regards raw kernels, the 34% of the sample shows a change of
269 slope, the 51% a maximum and a 15% neither of them. On the other hand the 70% of roasted
270 kernels shows a change of slope, the 18% a maximum and the 12% neither of them.

271 These results show a distribution, which is coherent with analogous results described in
272 (Delprete and Sesana, 2014). As stated above, the numerical values are therefore different as
273 a different moisture level is present in the examined sample and it is well known (Koyuncu et

274 al., 2004; Guner et al., 2003) that for wood and shells this property influences the mechanical
275 properties.

276

277

278 **3.1.4. CTA scans**

279 The digital geometry of Sample 6 specimens was obtained by means of General Electric
280 Phoenix V|tome|x m, a versatile X-ray micro-focus computed tomography system for 3D
281 metrology and analysis. It allows carrying out non-destructive testing tasks with less than
282 1 μm detail detectability. As stated above, the outer and the inner surfaces of the hazelnut
283 kernels were discretized with 0.4 mm resolution by the measurement system and then a re-
284 mesh process has led to a strong reduction of elements. In Figure 8 the external a) and
285 internal c) surfaces, supplied by computed tomography, and the same surfaces after the re-
286 meshing process b) and d) are reported as an example.

287

288 **Figure 8: External a) and internal c) surfaces by CTA and after re-meshing elaboration b) and d).**

289

290 **3.2. Numerical simulations**

291 As shown in Table 4, the elastic modulus values are distributed as a normal both for raw
292 kernels and roasted kernels, so it is possible to define a 95% level confidence interval for both
293 samples. In particular, as regards raw kernels, the lower and the upper limit are, respectively
294 6.4 MPa and 16.9 MPa. For each hazelnut kernel three simulations have been carried out, that
295 is three different values of elastic modulus have been considered: the lower limit, the mean
296 and the upper limit. In Figure 9 the simulation results are plotted along with the 95% limit
297 curves of Sample 2.

298

299 **Figure 9: Comparison between numerical results (black, red and green lines) and 95% limit curves (blue lines).**

300

301 The black, red and green curves are obtained, respectively, with the lower limit, the mean and
302 the upper limit stiffness values. The comparison of the curves outlines the influence of the
303 geometry of the kernel: for example the upper limit curve in case b) assumes lower values
304 with respect to case c). Moreover also the area delimited by the upper and lower limit curves
305 is very different from case b) to case c).

306 The upper limit curve (green curve) lies, in all cases, between the 95% limit curves (blue
307 curves) so it gives a good approximation of the compressive behavior of the hazelnut kernel;

308 the mean curve (red curve) is almost coincident with the lower limit curve and the lower limit
309 curve (black curve) lies out of the 95% range. So the stiffness values that better describe the
310 compressive behavior of the hazelnut are included in the upper part of the Gaussian
311 distribution.

312

313 **4. Conclusions**

314 A procedure to define a numerical model of kernel compression testing has been described.

315 The geometric model has been defined by means of 3 dimensional scanning of actual
316 hazelnuts. The constitutive material model has been selected according to experimental
317 evidence as linear elastic. The calibration parameters were obtained by means of processing
318 experimental data.

319 Experimental data acquisition and processing took a relevant time lapse as it allowed defining
320 many points as the sample size, the best experimental data fitting curve and corresponding
321 confidence interval, the simulation results reliability.

322 Experimental testing also pointed out that the compression of with and without pellicle
323 kernels outlined the influence of pellicle on mechanical behavior, that is, an increase of the
324 overall stiffness of the kernel. The affecting effect of moisture on compression mechanical
325 properties was confirmed.

326 The results show the influence of the geometry on the compressive behavior and outline an
327 underestimation of the elastic modulus; the underestimation is because the upper values of
328 the Gaussian distribution allow the numerical curves to lie between the 95% limit
329 experimental curves. This can be attributed to the approximation induced by the choice of a
330 perfect elastic material and to the great practical difficulty in extracting cylindrical kernel
331 specimen. A good approximation has been however achieved.

332

333 **Acknowledgments**

334 The research work was sponsored by PIEDMONT REGION within the ITACA Project (Lines
335 POR-FESR Axis 1: Innovation and production transition, Measure I.1.1: Innovative platforms
336 and POR-FEASR Axis 1: Improving the competitiveness of agriculture and forestry, Measure
337 124: Cooperation for development of new products, processes and technologies in agriculture,
338 food and forest sectors).

339 We gratefully thank Dr. Scatà and laboratory technicians of LABORMET DUE srl (Torino) for
340 precious help and counseling with CTA scanning.

341

342 **References**

343

344 ABAQUS 6.11-1. (2011). Analysis User's Manual.

345

346 AOAC (2000), Official Methods of Analysis, 17th Edn, no 925.40, Association of Official
347 Analytical Chemists, Washington, DC, USA.

348

349 Borges, A., Peleg, M. (1997). Effect of water activity on the mechanical properties of selected
350 legumes and nuts. *Journal of the Science of Food and Agriculture*, 75, 463-471.

351

352 Delprete C., Sesana, R. (2014). Mechanical characterization of kernel and shell of hazelnuts:
353 Proposal of an experimental procedure. *Journal of Food Engineering*, 124, 28-34.

354

355 Di Matteo, M., Albanese, D., Liguori, L. (2012). Alternative Method for Hazelnuts Peeling. *Food
356 and Bioprocess Technology*, 5, 1416-1421.

357

358 Donno, D., Beccaro, G.L., Mellano, G.M., Di Prima, S., Cavicchioli, M., Cerutti, A.K., Bononous, G.
359 (2013). Setting a protocol for hazelnut roasting using sensory and colorimetric analysis:
360 influence of the roasting temperature on the quality of Tonda Gentile delle Langhe cv.
361 Hazelnut. *Czech Journal of Food Sciences*, 31(4), 390-400.

362

363 Ercisli, S., Ozturk, I., Kara, M., Kalkan, F., Seker, H., Duyar, O., Erturk, Y. (2011). Physical
364 properties of hazelnuts. *International Agrophysics*, 25, 115-121.

365

366 FAO (2014) FAOSTAT. 2012 data. Food and Agriculture Organization of the United Nations,
367 Rome, IT.

368

369 Ghirardello, D., Contessa, C., Valentini, N., Zeppa, G., Rolle, L., Gerbi, V., Botta R. (2013). Effect
370 of storage conditions on chemical and physical characteristics of hazelnut (*Corylus avellana*
371 L.). *Postharvest Biology and Technology*, 81, 37-43.

372

373 Guidone, L., Valentini, N., Rolle, L., Me. G., Tavella, L. (2007). Early nut development as a
374 resistance factor to the attacks of *Curculio nucum* (Coleoptera: Curculionidae). *Annals of
375 Applied Biology*, 150, 323-329.

376

377 Güner, M., Dursun, E., Dursun, İ.G. (2003). Mechanical behavior of hazelnut under
378 compression loading. *Biosystems Engineering*, 85, 485–491.
379

380 Koyuncu, M.A., Ekinci, K., Savran, E. (2004). Craquing characteristics of walnut. *Biosystems*
381 *Engineering*, 87, 305–311.
382

383 Montgomery, M. C., Peck, E. A., Vining, G.G. (2001). Introduction to linear regression analysis.
384 John Wiley and Sons, New York, USA.
385

386 Ozdemir, F., Akinci, I. (2004). Physical and nutritional properties of four major commercial
387 Turkish hazelnut varieties. *Journal of Food Engineering*, 63, 341-347.
388

389 Saklar, S., Urgan, S., Katnas, S. (1999). Instrumental Crispness and Crunchiness of Roasted
390 Hazelnuts and Correlations with Sensory Assessment. *Journal of Food Science*, 64, 1015-1019.
391

392 Torchio, F., Giacosa, S., Río Segade, S., Mattivi, F., Gerbi, V., Rolle, L. (2012). Optimization of a
393 Method Based on the Simultaneous Measurement of Acoustic and Mechanical Properties of
394 Winegrape Seeds for the Determination of the Ripening Stage. *Journal of Agricultural and Food*
395 *Chemistry*, 60, 9006–9016.
396

397 Valentini, N., Rolle, L., Stevigny, C., Zeppa, G. (2006). Mechanical behavior of hazelnuts used for
398 table consumption under compression loading. *Journal of Science of Food and Agriculture*, 86,
399 1257–1262.
400

401 Winton, A.L. (1906). The microscopy of vegetable foods. John Wiley & Sons, New York, USA.
402

403 Young, W.J. (1912). A study of nuts with special reference to microscopic identification. US
404 Department of Agriculture - Washington, Govt. Print. Off., USA.

Figure1
[Click here to download high resolution image](#)

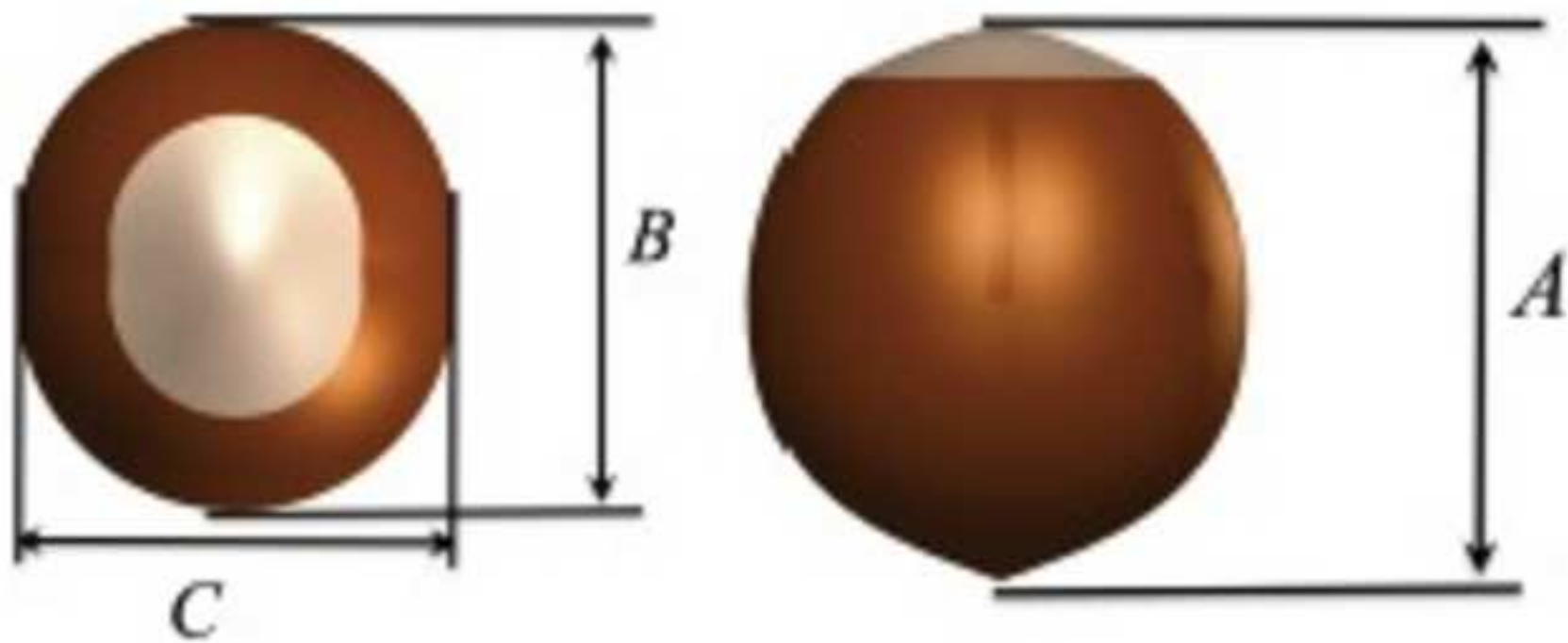


Figure 2
[Click here to download high resolution image](#)

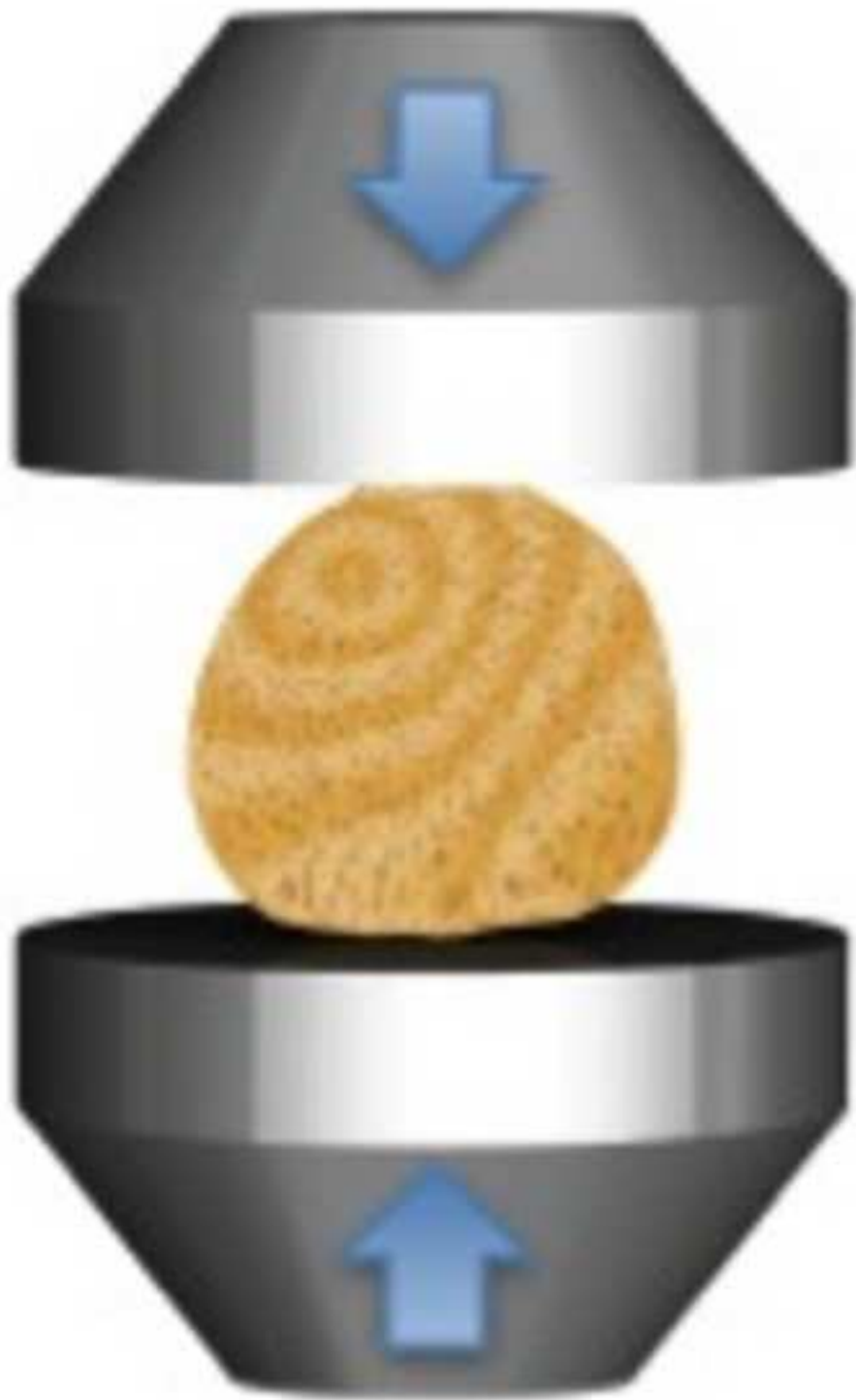


Figure 3
[Click here to download high resolution image](#)



Figure 4
[Click here to download high resolution image](#)

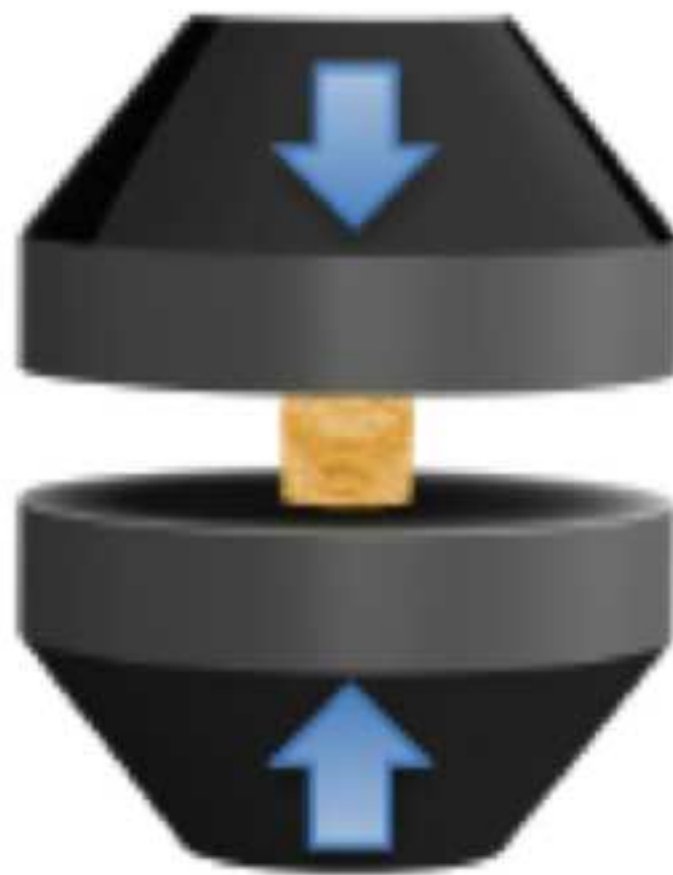
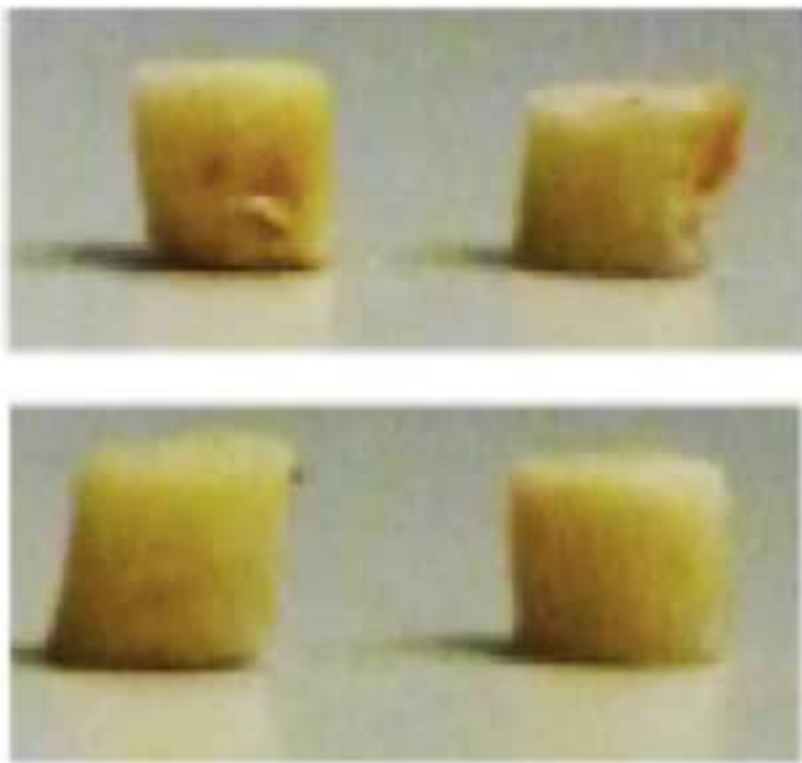


Figure 5
[Click here to download high resolution image](#)

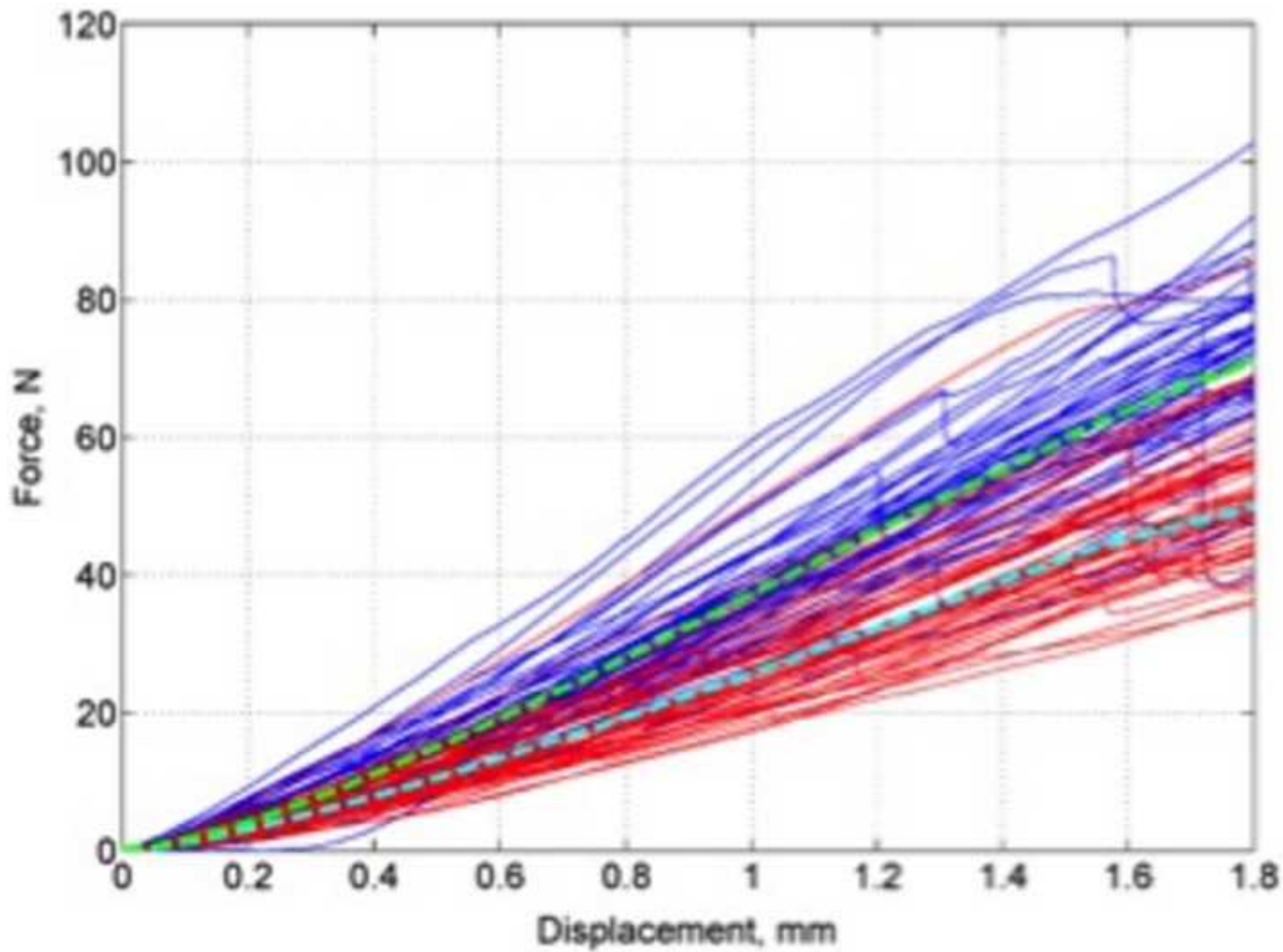


Figure 6
[Click here to download high resolution image](#)

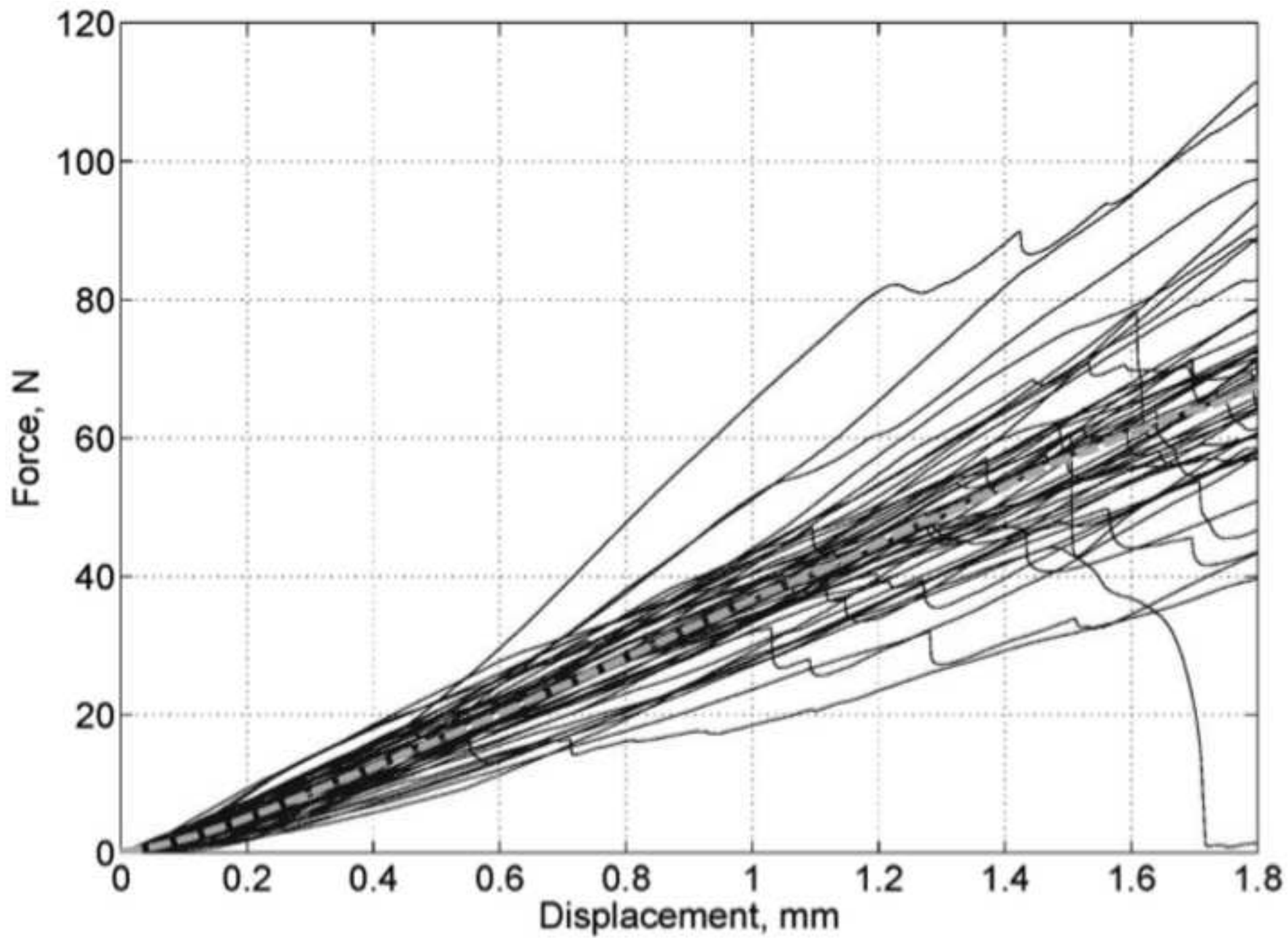


Figure 7
[Click here to download high resolution image](#)

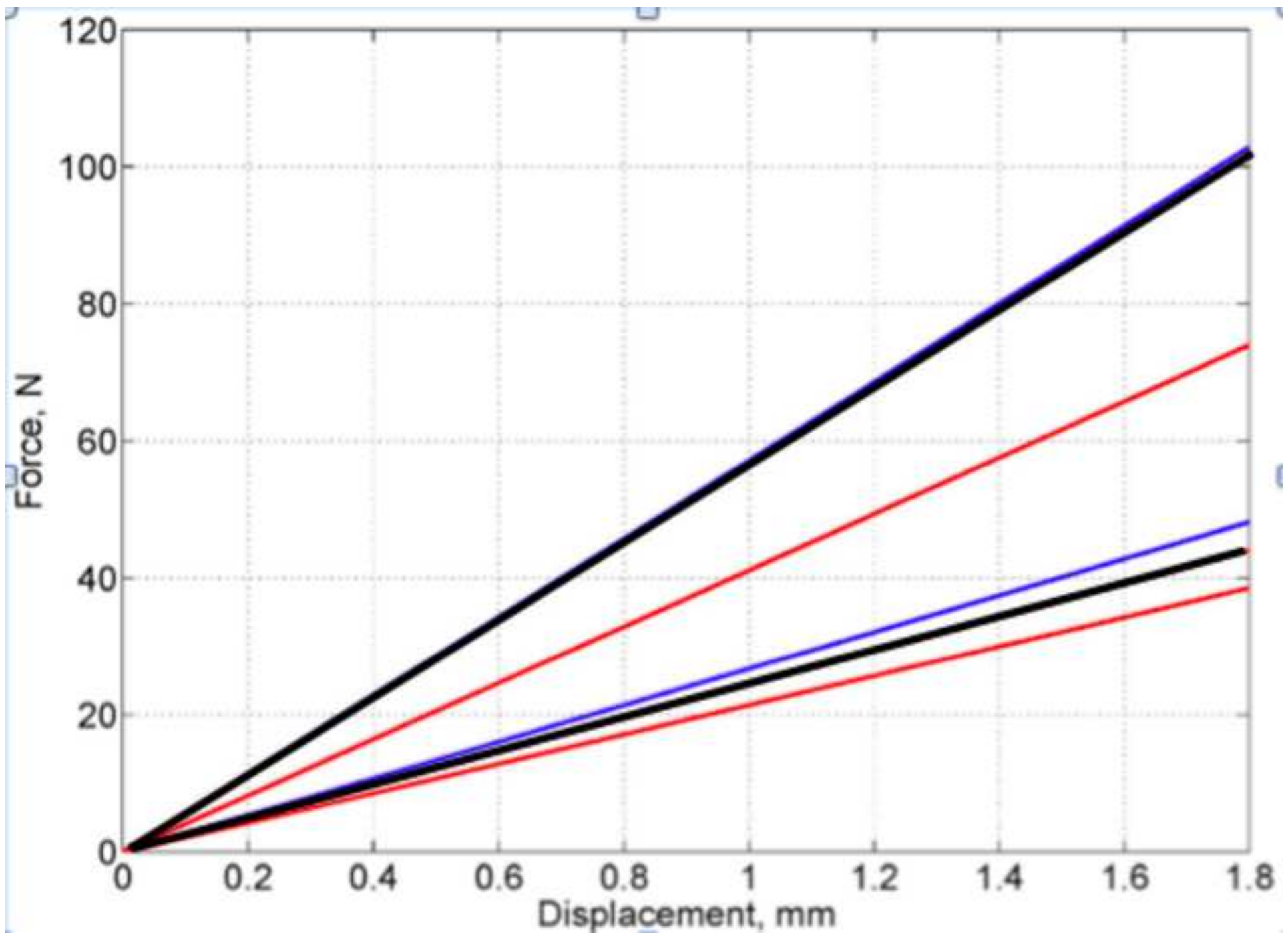
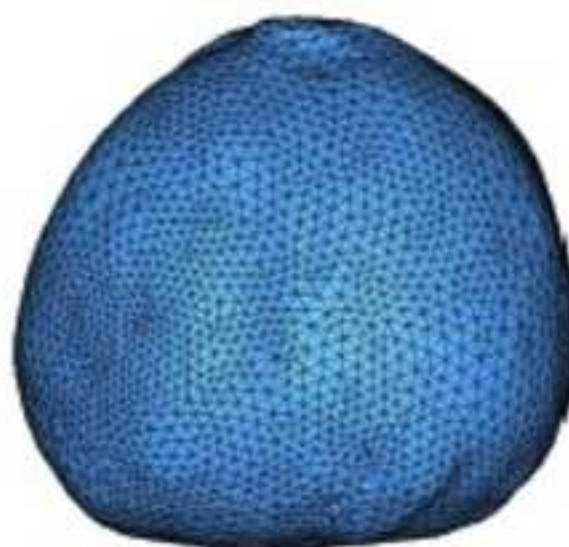


Figure 8
[Click here to download high resolution image](#)



a)



b)



c)



d)

Table 1: Elements and nodes of numerical hazelnuts.

CTA number	Nodes	Elements
1	20349	99144
2	15689	76868
3	14768	72014
4	25415	126489

Table 2

Table 2: Average values and standard deviations of physical and geometrical measurements on the specimen samples.

		Average value	Standard deviation	Minimum sample size
Mass [g]		1.27	0.08	43
Geometric parameters	<i>A/B [-]</i>	1.00	0.07	53
	<i>C/B [-]</i>	0.88	0.05	53
	<i>C/A [-]</i>	0.88	0.06	55

Table 3: Mechanical properties measurements on the whole kernel samples.

Sample	Kind of specimens		Average value	Standard deviation	Minimum sample size	χ^2 (85% conf. level)
1	Raw kernels with pellicle	Stiffness \bar{K} [N/mm]	41.93	7.75	42	positive
		\bar{L}_{kf} [N]	83.93	16.33	22	positive
2	Raw kernels without pellicle	Stiffness \bar{K} [N/mm]	31.25	5.02	39	positive
		\bar{L}_{kf} [N]	65.04	16.06	23	positive
3	Toasted kernels without pellicle	Stiffness \bar{K} [N/mm]	40.50	8.19	33	positive
		\bar{L}_{kf} [N]	78.64	29.79	18	positive

Table 4: Mechanical properties measurements on the kernel specimen samples.

Sample	Kind of specimens	Average value	Standard deviation	Minimum sample size	χ^2 (85% conf. level)	
4	Raw kernels	Elastic modulus \bar{E}_k [MPa]	11.61	2.68	46	positive
		Stress to failure UCS [MPa]	1.51	0.24	34	positive
		Knee stress σ_k [MPa]	1.23	0.21	27	positive
5	Toasted kernels	Elastic modulus \bar{E}_k [MPa]	10.81	3.43	53	positive
		Stress to failure UCS [MPa]	1.32	0.26	16	positive
		Knee stress σ_k [MPa]	1.12	0.30	41	positive

FIGURES:

Figure 1: Hazelnut shell and kernel main dimensions.

Figure 2: Kernel compression along A axis, experimental setup.

Figure 3: Compression failure of hazelnut kernel: cotyledon separation.

Figure 4: Kernel specimens a) and specimens compression setup b).

Figure 5: Force-displacement raw kernel curves with (blue) and without (red) pellicle.

Average curves are respectively the green and the cyan ones.

Figure 6: Force-displacement ~~toasted~~ roasted kernel curves with average curve (~~green~~ white).

Figure 6: Raw kernels with (blue continuous lines) and without (red continuous lines) pellicle and ~~toasted~~ roasted without (~~red dotted~~ black continuous lines) pellicle: 95% stiffness values limits.

Figure 7: External a) and internal c) surfaces by CTA and after re-meshing elaboration b) and d).

Figure 8: Comparison between numerical results (black, red and green lines) and 95% limit curves (blue lines).